

Parallel Digital Modem Using Multirate Digital Filter Banks

Ramin Sadr
F.-P. Vaidyanathan
Dan Raphaeli
Sami Tlinedi

August 15, 1994



National Aeronautics and
Space Administration

Jet Propulsion Laboratory
California Institute of Technology
Pasadena, California

Digital Modem Design Based on Multirate Filter Banks*

Ramin Sadr MEMBER, IEEE Dan Raphaeli MEMBER, IEEE
Sami Hinedi MEMBER, IEEE

November 23, 1994

Abstract

A new approach for the architecture of an all digital modem design is presented in this article. The key feature of this approach is a lower processing rate than the Nyquist rate (the input sampling rate) and even the symbol rate. The lower processing rate is achieved by the use of a parallel structure, based on multirate filter banks concepts. In our proposed scheme, matched filtering is implemented in the subbands of an analysis/synthesis filter bank. The modem architecture is particularly suited to high data rate applications, where the processing rate can be chosen independent of the speed of the integrated circuit technology. Possible applications of the PRX include giga-bit/second satellite channels, multiple access communication systems, optical links and interactive cable TV.

1 Introduction

With the evolution of high speed satellite and terrestrial communication, the applications for high data rate or wide-band communication systems are becoming abundant. Existing earth orbital missions such as the Telecommunication and Data Relay Satellite System (TDRSS)

*This work was performed at the Jet Propulsion Laboratory, California Institute of Technology, and was sponsored by the National Aeronautics and Space Administration.

supports data rates of 110 to 300 Mbps. Communications systems must today be 10 to 100 times faster and handle an ever rising data throughput.

Advances in digital integrated circuit (IC) technology has made switching speeds close to 1 GHz possible. However, the widespread use of high speed components is costly both in price and power consumption. One of the key bottlenecks in DSP design for an all-digital receiver is the availability of components (e.g., multiply-accumulator) that process each sample at the input sampling rate, when the latter can be 200 MHz or so. The objective here is to explore a cost effective solution to this problem. The ideal solution is to employ lower speed (50-70 MHz) components using IC technologies such as the Complementary Metal Oxide Semiconductor (CMOS) technology. CMOS has many known advantages such as low cost, low power, and high density. The data acquisition technology also has undergone rapid advancements, where today, one giga sample per second analog-to-digital (A/D) converters become available. By using a single high speed A/D component and a small number of high speed components (e.g., multiplexers only), a fundamental question is posed:

Is it possible to architect a digital receiver such that the processing rate is slower than both the sampling and the symbol rate?

The answer to the above question is "yes". In this work, we devise a new approach for designing a digital receiver that trades off processing rate with parallelism. Our presentation is largely based on the evolving disciplines of multirate signal processing and digital filter bank theory. Classically, the filter banks have been used for subband coding applications. Using the filter bank theory for designing the digital receiver, the overall system lends itself to a modular structure which can benefit the design and fabrication process of functional hardware. This modularity is due to the underlying structure of the receiver composed of finite impulse response (FIR) filters and two FFT blocks. The general approach has been successfully applied to wide band digital phase lock loops in [1]. This work formed the basis of the results presented here, and it was expanded to provide a cohesive approach to the

design of digital receivers. Our methodology is also suited for multi-channel communication applications such as multi-carrier modulation systems, multiple spacecraft communication (or users), and spread spectrum communication systems.

The ideal coherent receiver for detection of signals in Additive White Gaussian Noise (AWGN) is well known [9]. An all-digital version of this receiver is presently used in NASA's Deep Space Network (DSN) [3]. A simplified model for this digital receiver is depicted in Fig. 1, and is the basis for the development of the parallel receiver. The digital receiver architecture which will be developed here, referred to as the parallel receiver (PRX), demodulates and tracks the received symbol stream, and provides tracking for the carrier phase and the symbol timing. The IF input signal is sampled by a high speed A/D converter operating at a rate f_s and the samples are fed into a serial to parallel converter of size M . The signal then consists of a sequence of length M vectors sampled at the rate f_s/M . In each two consecutive vectors of size M are concatenated to form a length $2M$ vector. These vectors are then filtered to a sequence of subband signals (a vector sequence in which each vector component corresponds to one subband signal) by an analysis filter bank. The outputs of the parallelized matched filter is the symbol stream by denoted a_i . The outputs are available in parallel (the size $2M$ vectors are transformed back to size M vectors), which can be used for further parallel processing in carrier phase and bit timing synchronization.

The subband realization of the matched filter is a special case of a broader concept, which we refer to as *subband convolution*; see Fig. 2. In this figure, two signals, $x(n)$ and $q(n)$ are both divided into $2M$ subbands by separate analysis filter banks $\{H_k(z)\}$ and $\{P_k(z)\}$, $k = 0, \dots, 2M-1$. The filter bank used here is an under-decimated (non-maximally decimated) filter bank since there are $2M$ subbands, but the decimation and expansion rate is only M . The output of the filter bank is formed by the set of synthesis filters $\{P_k(z)\}$. The filter banks are designed in such a way that the output, $o(n)$, is equal to the result of the convolution of $x(n)$ with $q(n)$. Subband convolution using maximally decimated filter

banks has been previously proposed in [2], when the desired output is the convolution of two signals *decimated by M*. In our proposed method, the undecimated convolution appears at the synthesis bank output.

As a byproduct of the filter bank structure, the subbands signals can find various other uses such as: residual (or pilot) carrier tracking, extraction and/or recording of signals from various subbands, radio science for correlation of wideband sources.

2 A Digital Receiver Model

The received waveform $r(t)$ is composed of signal $s(t)$ plus noise $n(t)$, and can be written as

$$r(t) = \text{Re} \left\{ \sum_i a_i p(t - iT) e^{j2\pi f_c t + j\theta} \right\} + n(t), \quad (1)$$

where a_i is the symbol sequence in complex form, f_c is the carrier frequency, θ is the carrier phase and T is the symbol duration. Equation (1) applies to any two dimensional modulation, e.g. QAM (Quadrature Amplitude Modulation), MPSK (M -ary Phase Shift Keying).

The model for the digital receiver here is depicted in Fig. 1. We assume the availability of an intermediate stage for open loop or closed loop down-conversion of the RF signal to a convenient frequency for the A/D conversion, referred to as the intermediate frequency (IF). This implies that bandpass sampling [4] is used, at rate f_s . In bandpass sampling, a single A/D converter is used and the signal is demodulated to baseband by digitally multiplying it with an estimate of the carrier with frequency ω_c and phase θ produced by a Numerically Controlled Oscillator (NCO). The output of the NCO mixed with the signal is followed by a low-pass filter $B(z)$ to reject the double frequency components. A decimation by two or more is often possible at this point [6] to reduce the processing rate. We will omit this decimation operation since it is not relevant to our structure. A demodulator here consists of the mixer and the filter $B(z)$. The symbol rate is $1/T$ seconds, and the number of samples per symbol duration is equal to $D = Tf_s$, and is assumed to be an integer. In the actual system, the

sampling clock and the symbol clock may not be synchronized. In this case, the symbol timing synchronization may employ time varying matched filter [5]. The matched filter is represented as a filter $Q(z)$ followed by a decimator by D . All other required functions (e.g. residual phase error, $\Delta\phi$ indicators, power estimators) use the output of the matched filter. For the purpose of the symbol timing loop, matched filter outputs at mid-symbol position are required for the Digital Transition Tracking Loop (DTTL)[9]. This can be accomplished by simply having $D = T f_s / 2$ as the decimation ratio. We can combine the lowpass filter $B(z)$ and the matched filter $Q(z)$ to one filter $C(z) = B(z)Q(z)$ if desired. It is exhibited here that treating these filters separately yields a less complex realization.

2.1 Description of the PRX

The PRX block diagram is shown in Fig. 3. All the digital filters mentioned in this article are Finite Impulse Response (FIR) filters. The input signal to the PRX consists of a sequence of length M vectors sampled in rate f_s/M . Every two consecutive vectors of size M are concatenated to a length $2M$ vector. Each component is mixed with a carrier reference $\pm \cos 2\pi n$ each subband, and then filtered by one of the polyphase components of the analysis filter $H(z)$ denoted by $E_k(z^2)$. The resulting sequence of vectors are processed by an IFFT (Inverse Fast Fourier Transform) block. By appropriate selection of subbands from the analysis filter bank, a lowpass frequency characteristic can be realized, as further described in Section 3. In Fig. 3, the filter $G_k(z)$, performs the subband matched filtering, as outlined in Section 4. The output vectors are processed by an FFT block and each component is processed by the polyphase of the synthesis filter, denoted here by $R_k(z^2)$. The output vector of length $2M$ $\mathbf{v}'(n)$ is combined to form a length M vector, $\mathbf{v}(n)$, by $\mathbf{v}_k(n) = \mathbf{v}'_{k+M}(n) + \mathbf{v}'_k(n-1)$. The sequence of vectors $\mathbf{v}(n)$ forms the parallel output of the matched filter, and it is generated at the lower rate f_s/M . It is noted that if M is not a multiple of D , then the components of this subset as well as the cardinality of the subset

are periodically time varying. The expansion decimation operation at the output section of Fig. 3 can be regarded as an interleaver and there is a one-to-one correspondence between the components of $\{v(n)\}$ and the desired sequence of symbols. When M is a multiple of D , the symbol sequence a_i has a one-to-one correspondence with a subset of the parallel outputs. Otherwise, refer to Section 4.2 for a different realization of the interleaver in which a commutator (parallel to serial converter) can be used instead of expanders. This is desirable when a serial symbol output stream is required.

3 Parallel Architecture for Demodulator Using Filter Banks

The demodulator consists of a mixer for mixing the input with the carrier signal, followed by a lowpass filter $B(z)$ to reject the double frequency images. Consider a filter bank, covering the full band $(0, 2\pi]$. Let each subband be multiplied by a coefficient δ_k which can take the values 0 or 1. We can discard a set of subbands, by choosing $\delta_k = 0$ for this set. The remaining subset constitutes the passband of the $(0, 2\pi]$ system, and the discarded set constitutes the stopband. We refer to our filtering problem here as a "partial band reconstruction" [7] as opposed to perfect reconstruction in which case the objective is to reconstruct the signal around the whole unit circle. We impose here an additional constraint that the signal outside the reconstruction band is arbitrarily suppressed. Our problem is a special case of a multilevel tunable filter design, where each subband is given an arbitrary weight (δ_k).

Typically, there are three sources of distortion in filter banks, these are: aliasing, amplitude distortion, and phase distortion. As shown in [7], alias cancellation is not possible in a maximally decimated filter bank if only a subset of the subbands are used in signal reconstruction. Aliasing introduced due to dropping of subbands in a maximally decimated filter bank is illustrated in Fig. 4. In this figure, a subset of real synthesis filters $P_k(z)$, for which $7 < k$

or $i > k+2$ are discarded. The aliasing error in the signal is not canceled in the frequency bands where the adjacent synthesis filters are discarded. In our proposed structure, aliasing is suppressed (not canceled) by the use of underdecimated filter bank. In this system, $2M$ subbands are used, each decimated by M , so there is ample space for the rejection of the images. Amplitude distortion and phase distortion (in the partial band) are minimized by a proper choice of analysis and synthesis filters.

Let $\{H_k(z)\}$ and $\{P_k(z)\}$, $k = 0, \dots, 2M-1$ be two sets of FIR filters. The filters $\{H_k(z)\}$ are called analysis filters, $\{P_k(z)\}$ are called synthesis filters, and let $W_{2M} = \exp\{-j\frac{2\pi}{M}\}$. The filterbank is called a discrete Fourier transform (DFT) analysis/synthesis filter bank if $H_k(z) = H_0(zW_{2M}^k)$ and $P_k(z) = P_0(zW_{2M}^k)$, i.e., all filters are a frequency shifted version of one prototype, $H_0(z)$ or $P_0(z)$.

In general, the subband filter pairs $\{H_k(z), P_k(z)\}$ have complex coefficients. However, it can be shown that for a DFT filter bank, configured for partial band reconstruction, with a symmetric arrangement of the subbands around the zero frequency results into a real-valued impulse response for the overall system. If $H_0(z)$ is real, we can keep an odd number of subbands $2M-p, 2M-p+1, \dots, 2M-1, 0, 1, \dots, p$ and obtain a real-valued lowpass response with cutoff frequency of approximately

$$\omega_p = (2p+1)\pi/2M. \quad (2)$$

Note that the cutoff frequency can be easily tuned (with a coarse resolution) by choosing p .

Let $X(z)$ be the z -transform of the input $x(n)$ of the filter-bank, and $O(z)$ be the z -transform of its output. The decimator-expander after each filter $H_k(z)$ generates images of the subband signal $H_k(z)X(z)$. The $M-1$ images are replicas of the signal, shifted in frequency by multiples of $2\pi/M$. The filter $P_k(z)$ then passes only the signal $H_k(z)X(z)$ and rejects the images. Let $W = \exp\{-j\frac{2\pi}{M}\}$. Formally, the signal at the output of the filter

bank can be expressed as [8]

$$O(z) = \sum_{i=0}^{M-1} A_i(z) X(z W^i), \quad (3)$$

where $A_i(z)$ is the alias transfer function, and is defined as

$$A_i(z) = \frac{1}{M} \sum_{k=0}^{2M-1} \delta_k H_k(z W^i) P_k(z) \quad (4)$$

The filterbank is called alias free if $A_i(z) = 0$ for $i \neq 0$. As shown in Fig. 5a (the filter $P(z)$ in the figure will be used later), $P_0(z)$ and $H_0(z)$ can be designed such that the stopband of $P_0(z)$ covers the frequency support of the images $H_0(z W^i)$, $i = 1, \dots, M-1$. With a sufficient stopband attenuation, we can assume

$$H_0(z W^i) P_0(z) \approx 0 \quad (5)$$

Since all the filters are shifted replicas of a single prototype, it is evident that $A_i(z) \approx 0$, $i \neq 0$, hence the system is approximately alias free. The amount of alias distortion can be as small as desired by designing filters with sufficiently high stopband attenuation. Furthermore, monotonically increasing stop band attenuation (non-equal ripple stopband) is a desired property, since it results into further rejection of distant images from the filter cutoff frequency. This property insures that only the neighboring filters contribute to the aliasing distortion. In the maximally decimated filter bank, aliasing is eliminated by cancellation of the alias components, when adding the outputs of the synthesis filters. Since there is no such alias cancellation in a non-maximally decimated filter bank, discarding synthesis filters do not cause distortion, i.e., the phenomena illustrated in Fig. 4 does not occur.

Using the assumption that the system is alias free, the input-output transfer function $T(z)$ is

$$T(z) = \frac{1}{M} \sum_{k=0}^{2M-1} \delta_k H_k(z) P_k(z). \quad (6)$$

Any lowpass filter with cutoff frequency $\pi/2M$ and good frequency response may be chosen for $K(z) = H_0(z)P_0(z)$ to form multilevel response. However, in the transition bands, where adjacent filters overlap, the overall frequency response may exhibit dips or bumps. The ideal choice for $K(z)$ is to satisfy the Nyquist($2M$) property. Formally, $H(z)$ is a Nyquist(M) filter [8] if

$$h(Mn) = c\delta(n), \quad (7)$$

where c is a constant and $\delta(n)$ is the Kronecker delta function. Let us assume $c = 1/M$, then $K(z)$ is a Nyquist($2M$), then

$$\sum_{k=0}^{2M-1} K(zW_{2M}^k) = 1. \quad (8)$$

In the frequency region where $K(zW_{2M}^k)$ and $K(zW_{2M}^{k+1})$ overlap, it is assumed that the remaining terms in (8) are negligible, this yields $K(zW_{2M}^k) + K(zW_{2M}^{k+1}) \simeq 1$. This implies that in the system passband, where $\delta_k = 1$, the frequency response is flat. Furthermore, if we are implementing a multilevel filter, in the region where the subbands overlap we have

$$\delta_k K(zW_{2M}^k) + \delta_{k+1} K(zW_{2M}^{k+1}) \simeq \delta_k + (\delta_{k+1} - \delta_k) K(zW_{2M}^{k+1}). \quad (9)$$

Thus, if the gain of $K(z)$ in its transition band is monotonically decreasing, then the gain of the multilevel filter at the transition region between the level δ_k and the level δ_{k+1} is also monotonic.

3.1 Efficient DFT Filter Banks Implementation

The DFT filter bank is efficiently implemented as follows. We express the prototype filters in polyphase representations as

$$H_0(z) = \sum_{i=0}^{2M-1} P_i(z^{2M}) z^{-i}, \quad (10)$$

$$P_0^k(z) = \sum_{i=0}^{2M-1} P_i(z^{2M})z^i \quad 1$$

The analysis filters can then be expressed as

$$H_k(z) = H_0(z)W_{2M}^k = \sum_{i=0}^{2M-1} (z^{-1}W_{2M}^k)^i P_i(z^{2M}) \sum_{i=0}^{2M-1} z^i P_i(z^{2M}) W_{2M}^{k,i} \quad (12)$$

Noble identity [8] can be used to move the decimation by M before the polyphase filters, and an efficient structure for the analysis DFT filter bank is realized. The operation in Fig. 3, denoted by \mathbf{W}^* is a matrix multiplication with the DFT matrix conjugated (same as it is inverse up to a constant), and is realized in practice by an FFT (inverse Fast Fourier Transform).

A representation as in (2) can be stated also for the synthesis filter $P_k(z)$. Note that a delay of $M-1$ must be added for causality. It is noted that real coefficients prototype yields real coefficients polyphase filters. Real valued polyphase filters can also be obtained using Generalized DFT (GDFT) filter banks [9].

Further reduction of the DFT computation complexity for the synthesis section can be achieved by making use of the fact that the number of outputs is less than the number of inputs. Let $g = \text{gcd}(D, M)$, then as latter shown in Section 4.2, only $2\hat{M} = 2M/g$ outputs are needed out of $2M$. In general the DFT formula is

$$X(k) = \sum_{n=0}^{2M-1} x(n) W_{2M}^{kn}, \quad (13)$$

for $k = 0, g, \dots, (2\hat{M}-1)g$, the DFT formula can be stated as

$$X(kg) = \sum_{n=0}^{2\hat{M}-1} \sum_{i=0}^{g-1} x(2\hat{M}-1+n+in).$$

Hence, only an FFT of size $2\hat{M}$ is required for the DFT computation of the synthesis section.

4 Matched Filter Implementation in the Subbands

Consider the PRX block diagram shown in Fig. 3. In this section we find a set of filters $G_0(z), \dots, G_{2M-1}(z)$, to operate on the subband signals, such that the overall response of the system approximates the matched filter $Q(z)$ (apart from the mixing operation). We begin by assuming that none of the subbands are discarded. After implementing $Q(z)$ in the subbands, the additional lowpass response $B(z)$ can be realized by dropping subbands, as described in the previous section. Note that it is possible to choose $Q(z) = C(z)$ and keep all the subbands. However, this choice results into a significantly higher complexity, since $Q(z)$ would have much higher order than the original matched filter, and furthermore, all the filters $\{G_k(z)\}$ would then have to be implemented, instead of a subset of these filters.

The system of Fig. 3 is developed as a special case of the subband convolution as shown in Fig. 2. In our case, $g_k(n)$, the decimated subbands of $q(n)$ constitute the impulse responses of the filters $G_k(z)$ shown in Fig. 3. Since $Q(z)$ is known a priori, the impulse responses $g_k(n)$ are precomputed and stored for use in real-time. It remains to show that with an appropriate choice of the filters in the system of Fig. 1, we can approximate the convolution result of $q(n)$ and $x(n)$ at the output with arbitrary accuracy. Recall that we use DFT filter banks, i.e., $H_k(z) = H_0(zW_{2M}^k)$, $P_k(z) = P_0(zW_{2M}^k)$ and $P_k(z) = P_0(zW_{2M}^k)$.

The decimated subbands of $x(n)$, $u_k(n)$ and the decimated subbands of $q(n)$, $g_k(n)$, can be expressed in the z -domain as

$$U_k(z) = \frac{1}{M} \sum_{i=0}^{M-1} X(z^{1/M} W^i) H_k(z^{1/M} W^i), \quad (15)$$

and

$$G_k(z) = \frac{1}{M} \sum_{i=0}^{M-1} Q(z^{1/M} W^i) P_k(z^{1/M} W^i). \quad (16)$$

Thus, the output of the system is

$$O(z) = \sum_{k=0}^{2M-1} P_k(z) U_k(z^M) G_k(z^M) =$$

$$= \frac{1}{NM^2} \sum_{k=0}^{2M-1} P_k^i(z) \left(\sum_{i=0}^{M-1} X(zW^i) H_k(z) \right) \left(\sum_{j=0}^{M-1} Q(zW^{-j}) P_k(z) \right) \quad (17)$$

After some manipulations, $O(z)$ can be expressed as

$$O(z) = \sum_{i=0}^{M-1} \sum_{j=0}^{M-1} X(zW^i) Q(zW^j) A_{i,j}(z), \quad (8)$$

where

$$A_{i,j}(z) = \frac{1}{M^2} \sum_{k=0}^{2M-1} H_k(zW^i) P_k(zW^j) P_k^i(z). \quad (19)$$

We can define the system to be alias free

$$A_{i,j}(z) = 0 \quad \text{for } i + j \neq 0 \quad (20)$$

the system is alias free and there is no distortion, i.e.,

$$A_{0,0}(z) = \frac{1}{M^2} \sum_{k=0}^{2M-1} H_k(z) P_k(z) P_k^i(z) = \quad (2)$$

then the output is the desired convolution of $x(n)$ with q non non-maximally decimated filter bank system, one can obtain alias suppression by designing prototype filters such that

$$H_0(zW^i) P_0(zW^j) P_0^i(z) \approx 0 \quad \text{for } i + j \neq 0. \quad (22)$$

Condition (21) implies that the filter $K(z) = H_0(z) P_0(z) P_0^i(z)$, must also be Nyquist(2π) as in (8)

A simple procedure for designing the prototype filters is proposed here. Many other procedures can be applied to this filter design problem, some of these can be found in [8]. In particular, nonlinear optimization can be applied, in which case the objective function is obtained directly from the conditions (22) and (21).

The output symbols a obtained in parallel form sufficient statistics for synchronization, lock detection, SNR estimation, equalization and soft decoding. Various approaches are

available for symbol timing synchronization that may be used for the PRX, such as digital transition tracking loop [23] which can easily be incorporated into the system; this loop may directly use the parallel outputs of the interleaver [15]. Suppressed carrier tracking can also be implemented in parallel as a trivial extension of the conventional Costas loop, as outlined in [15].

4.1 A simple design procedure

Let Ω_H , Ω_P and Ω_F be the stopband frequencies of the filters $H_0(z)$, $P_0(z)$ and $P'_0(z)$ respectively as illustrated in Fig. 5a. These filters are assumed to be linear phase lowpass filters. For a sufficiently high stopband attenuation, condition (22) is satisfied if the following set of conditions is simultaneously satisfied:

$$\begin{cases} \Omega_H + \min(\Omega_F, \omega_{-1}^n) \leq \frac{2\pi}{M} \\ \Omega_P + \min(\Omega_H, \omega_{-1}^n) \leq \frac{2\pi}{M} \\ \Omega_P + \min(\Omega_H, \omega_{-1}^n) \leq \frac{2\pi}{M} \end{cases} \quad (23)$$

or, equivalently, if

$$\min(\Omega_H, \Omega_P) + \max(\Omega_H, \Omega_P, \Omega_F) \leq \frac{2\pi}{M} \quad (24)$$

Among the prototypes $\{H_0(z), P_0(z)\}$, the order of the filter $P_0(z)$ has the highest contribution in the total system complexity for the following reasons: 1. $G_k(z)$ has complex coefficients. 2. The number of nonzero coefficients in $g_k(n)$ is $1/M$ times the order of $Q(z)P_0(z)$ compared to $1/2M$ times the order of $H_0(z)$ for $P'_0(z)$. For minimizing the order of this filter, it is desirable to widen its transition band as much as possible. Between the filters $P'_0(z)$ and $H_0(z)$, the one with the narrower bandwidth is chosen to be $H_0(z)$. This choice provides the minimum amount of overlap between the subbands for applications that process the subbands signals separately. The lowest complexity choice for Ω_P is to make it as large as Ω_P . Moreover, we can set $P_0(z) = P'_0(z)$ for simplicity. Then, the filters are designed with the condition $\Omega_P + \Omega_H = \frac{2\pi}{M}$.

Condition (21) is satisfied approximately by designing $H_0(z)$ to be Nyquist($2M$), and designing $P_0(z)$ and $P_0(z)$ to have linear phase and wide passband with low ripple, which is wide enough to cover the transition band of $H_0(z)$. In the causal form of the prototype filters, care must be taken to force the group delay of these filters to be a multiple of M . An example of a filter bank design for $M = 3$ is shown in Fig. 5b. In this example, the order of $H_0(z)$ is 35 and the order of $P_0(z) = P_0(z)$ is 23. The aliasing error from (19) can be defined as

$$\max_{m,n} \int_0^{2\pi} |A_{m,n}(e^{j\omega})|^2 d\omega = \frac{1}{\pi M^3} \max_{m,n} \int_0^{2\pi} |H_0(e^{j\omega}W^m)P_0(e^{j\omega}W^n)P_0(e^{j\omega})|^2 d\omega \quad (25)$$

with $n + m \neq 0$. In the example of Fig. 5b, the maximum is obtained at $n = m = 1$, and the aliasing error is 54 dB which is well below the quantization noise floor for an 8-bit A/D converter.

4.2.1 Symbol Scheduling Generation From the Parallel Output

The expansion-decimation operation at the output section of Fig. 3 shows the correspondence between the components of $\{\mathbf{V}(n)\}$ and the desired sequence of symbols. When M is a multiple of D , the symbol sequence a_i has a one-to-one correspondence with a subset of the parallel outputs. When M is not a multiple of D , an alternative realization of the PRX output is derived here in which a commutator (parallel to serial converter) circuit can be used and expansion to a higher rate is not required. This is especially important if a serial symbol output stream is desired.

Let g denote the greatest common divisor (gcd) of M and D . Then, there exists \hat{M} and \hat{D} such that $M = g\hat{M}$ and $D = g\hat{D}$. Since \hat{M} and \hat{D} are relatively prime, there exist integers n_0 and n_1 such that $n_0\hat{M} + n_1\hat{D} = 1$. It can then be shown that the PRX output can be re-organized as shown in Fig. 6a. Next, define $r_i = m_1 + i\hat{M}$ and $l_i = \lfloor \frac{in_1}{\hat{M}} \rfloor$, i.e.,

the integer part of $\frac{n_1}{M}$; then, the following identity is valid

$$z^{-L_1 - \hat{M} \cdot r_1} z^{-n_1}. \quad (26)$$

Since $\gcd(n_1, \hat{M}) = 1$ then $r_i \neq r_j \forall i \neq j$. Hence, the implementation shown in Fig. 6b follows. Note that the value of some of the delays in this figure are negative (either n_0 or n_1 has to be negative), and in this case some delay must be added to the system for causality. The expansion-delays-decimation has been reduced to constant delays, a commutator circuit, and a routing switch.

5 Simulations and Tests

The system has been simulated for the case of sixteen bands ($M = 8$) by COMDISCO's Signal Processing Workstation software which supports the simulation of digital signal processing systems. The filters were designed according to Section 4.1.

The approach taken here for designing $H_0(z)$ is windowing the impulse response of an ideal filter. The window chosen here is the Hamming window, which provides a smooth response and a non-equal ripple stop band. It must be noted that by choosing the bandwidth of the ideal filter to be $\pi/2M$, the resulting filter is forced to be Nyquist($2M$), independent of the window shape used for designing the filter. The filter $P_0(z) = P_0(z)$ was designed as linear phase and a wider passband than $H_0(z)$. With filter lengths of $12M + 1$ for $H_0(z)$ and $8M + 1$ for $P_0(z)$ (the maximal order of $P_k(z)$ is 6 and the maximal order of $R_k(z)$ is 4), better than 60 dB attenuation is achieved in the stopband.

Number of experiments have been undertaken to verify the performance of PRX and are discussed and presented in detail in [11]. A brief description of two of these experiments is described here as follows: *a. Mean Square Error (MSE) Measurement:* In order to quantify the implementation error, in this simulation the Mean Square Error (MSE) criteria is used. The filter bank implementation error of the matched filter is measured by simulation. In this

Table 1: MSE Measurements

$01(1(1-11(z))$	$01(1(1(1-11(2-)),)) (2)$	MSE
$12M - 1$	$8M$	$1.27 * 10^{-5}$
$16M - 1$	$12M$	$8.17 * 10^{-6}$

experiment, none of the subbands are discarded. A random bipolar pulse stream is applied simultaneously to a sliding window filter ($Q(z) = 1 + z^{-1} + z^{-2} + z^{-3}$) and to the filter-bank implementation of the same filter. The difference signal between the two output signals is computed, and the average power of the "0101" sequence is measured. This provides a MSE measurement (the output power of the matched filter is normalized to unity). The very small MSE affirms the negligible loss in the bit error rate (BER) measurement. The MSE is tabulated in Table 1. *b. BER Measurement with Bandpass Sampling:* In this simulation, an IF modulated "1111" signal with rectangular pulse shape over the additive white Gaussian noise channel is simulated. The BER result is compared to the ideal theoretical BER when four complex samples per symbol are used for detecting the symbols. The Bandwidth-bit-time (BT) product of the simulated anti-aliasing analog filter is 1.5. The results are shown in Fig. 7. Note that the degradation shown in Fig. 7 is due only to the low number of samples per symbol (the same degradation results in the conventional implementation [5]).

6 Alternative Architectures

Our design problem can be reduced to the parallel implementation of a system composed of a FIR filter $C(z)$ followed by a decimator of rate D , at a lower rate than the output rate. Here we investigate two additional approaches to this problem, and make a comparison on the relative complexity of all three approaches.

Let M denote the decimation ratio between the input sampling rate and the processing

1st. For simplicity we assume that M is multiple of D . Let L be the order of $C(z)$. Here, we consider three options, namely:

1. Blocked Digital Filter [8]: the input is vectorized to length M vectors at a rate f_s/M by a serial to parallel converter. The vectors are then processed by a block filter $\mathbf{H}(z)$, which is a $M \times M$ matrix transfer function, that is each component of the matrix is a filter. The decimation by D at the output translates to the implementation of only M/D rows of the matrix. The matrix $\mathbf{H}(z)$ is pseudocirculant [8] which means that all the rows are cyclic rotations of the first row, with z^{-1} multiplies the element below the diagonal. The first row is given by $\mathbf{H}_{0,l}(z) : P_l(z)$, where $P_l(z)$ are the polyphase components of $C(z)$.
2. Frequency domain convolution: using a FFT to perform the convolution between $x(n)$ and $c(n)$. This approach has been classically used to compute linear convolutions and is referred to as the “overlap and save” method [10]. The input stream is divided to overlapping blocks of size $M + L - 1$ with $L - 1$ samples overlap, an FFT is performed on the block. The output is multiplied with the transform of $c(n)$ and transformed back to the time domain by IFFT. The first M coefficients are useful results, and the rest are discarded.
3. Filter bank approach: the filter bank structure derived in Section 4.

Next, the computational complexity of each option is stated in terms of the number of multiplication operations per sample at the low sampling rate.

In option 1, the matrix filtering entails a total of $M - 1$ multiplications with non-zero constants. As mentioned, only $1/D$ of the rows need to be implemented, leading to a reduction of the complexity by the same factor.

In option 2, the frequency domain convolution requires two FFT's of size $M + L$, and $M + L$ additional multiplications. The FFT requires approximately $\frac{1}{2}(M + L) \log_2(M + L)$

Table 2: Computational requirements of several options.

Option	Operations
1. Block Digital Filtering	LM/D
2. Frequency Domain	$(M + L) \log_2(M + L) + M + L$
3. Filter Bank	$20M + 8M/D + M \log_2 2M + 2M/D \log_2 2M/D + L'$

multiplications.

In option 3, The complexity of the filter bank approach is approximated by assuming that the order of $P_0(z)$ and $P_0(z)$ is $8M$ and the order of $H_0(z)$ is $12M$. These approximations have been derived empirically and represent a rough figure for the order of the filter bank to have very low distortion). The total complexity of the polyphase components of $H_0(z)$ is equal to the complexity of implementing $H_0(z)$ itself that is $12M$ multiplications. The same applies to $P_0(z)$, but only $1/D$ of the polyphase components need to be implemented. The order of each subbands filter is about $\frac{1}{M} L' + 8M$, where L' is the order of $Q(z)$ and is smaller than L . There are about M such filters (the rest of the $2M$ subbands are discarded). There is one FFT of size $2M$ and one of size $2M/D$. The result for the three options is summarized in Table 2.

In Fig. 8, each option is represented as a subspace in the two dimensional plane whose coordinates are L and M . In this comparison, $L' = L$ (in favor of option 3) and $D = 2$. Each subspace represents the range of variables L and M that yield minimal complexity among the three options. For a small L , the block digital filtering results into the lowest number of operations, but the benefits of the filter bank structure are lost. Also note that the case of M multiple of D is in favor of option 1.

7 Conclusion

In this article, we succeeded in formulating an architecture for a digital receiver such that the processing rate in the digital signal processing hardware is arbitrarily selected by the designer. Based on the concept of subband convolution using a multirate filter bank, an architecture was devised that operates in parallel at an arbitrary low rate. The detected symbol stream is directly output from the subbands in parallel. Various options, for the implementation of the overall receiver was studied and their associated complexities was assessed. Simulation of the PRX architecture verifies that there is no loss associated in PRX when compared to the classical implementation of the receiver.

Acknowledgments: We acknowledge Prof. P.P. Vaidyanathan of California Institute of Technology for his contributions and insights in developing this work

References

- [1] Sadr R., Shah B., Himedi S., "Parallel Digital Phase Lock Loop Employing Multirate Digital Filter Banks", Submitted for Publication to IEEE Trans. on Comm., May 1994.
- [2] Vaidyanathan P.P., "Orthonormal and Biorthonormal Filter Banks as Convolvers, and Convolutional Coding Gain, IEEE Trans. on Signal Processing, Vol. 41, No. 6, June 1993.
- [3] Himedi S., "NASA's Next Generation Deep Space Network Breadboard Receiver", IEEE Trans. Comm., Vol. 41, No. 1, January 1993.
- [4] Sadr R., Shahshahani M., "On Sampling Band-Pass Signals", TDA Progress Report 42-96, Jet Propulsion Laboratory, CA, Oct.

- [5] Sadr R., "Detection of Signals by the Weighted Integrate-and-Dump Filter", TDA Progress Report 42-91, Jet Propulsion Laboratory, Sept. 1987.
- [6] Sadr R., Hurd W., "Carrier Demodulation for the Advanced Receiver", TDA Progress Report 42-93 Jet Propulsion Laboratory, CA, Oct. 1988
- [7] Nguyen H. Q., "Partial Spectrum Reconstruction Using Digital Filter Banks", IEEE Trans. Signal Processing, Vol. 41, No. 9, September 1993.
- [8] Vaidyanathan P. P., *Multirate Systems and Filter Banks*, NJ: Prentice Hall, 1993.
- [9] Simon M.K., Hinedi S. and Lindsey W. C., *Digital Communication Techniques - Signal Design and Detection*, NJ: Prentice Hall, 1994.
- [10] Crochiere R.E., Rabiner L.R., *Multirate Digital Signal Processing*, NJ: Prentice Hall, 1983.
- [11] Sadr R., Raphaeli D., Vaidyanathan P. P., Hinedi S., "Parallel Digital Modem Using Multirate Filter Banks", J111, External Report, NASA, No. 94-12, Aug. 1994.

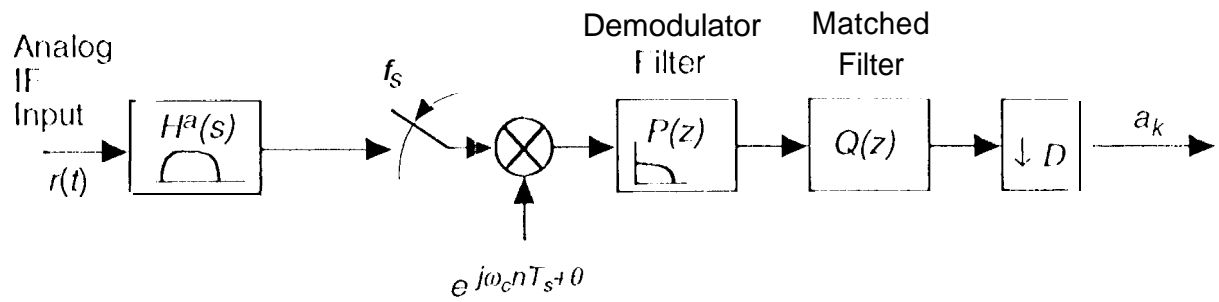


Figure 1. Digital Receiver Model

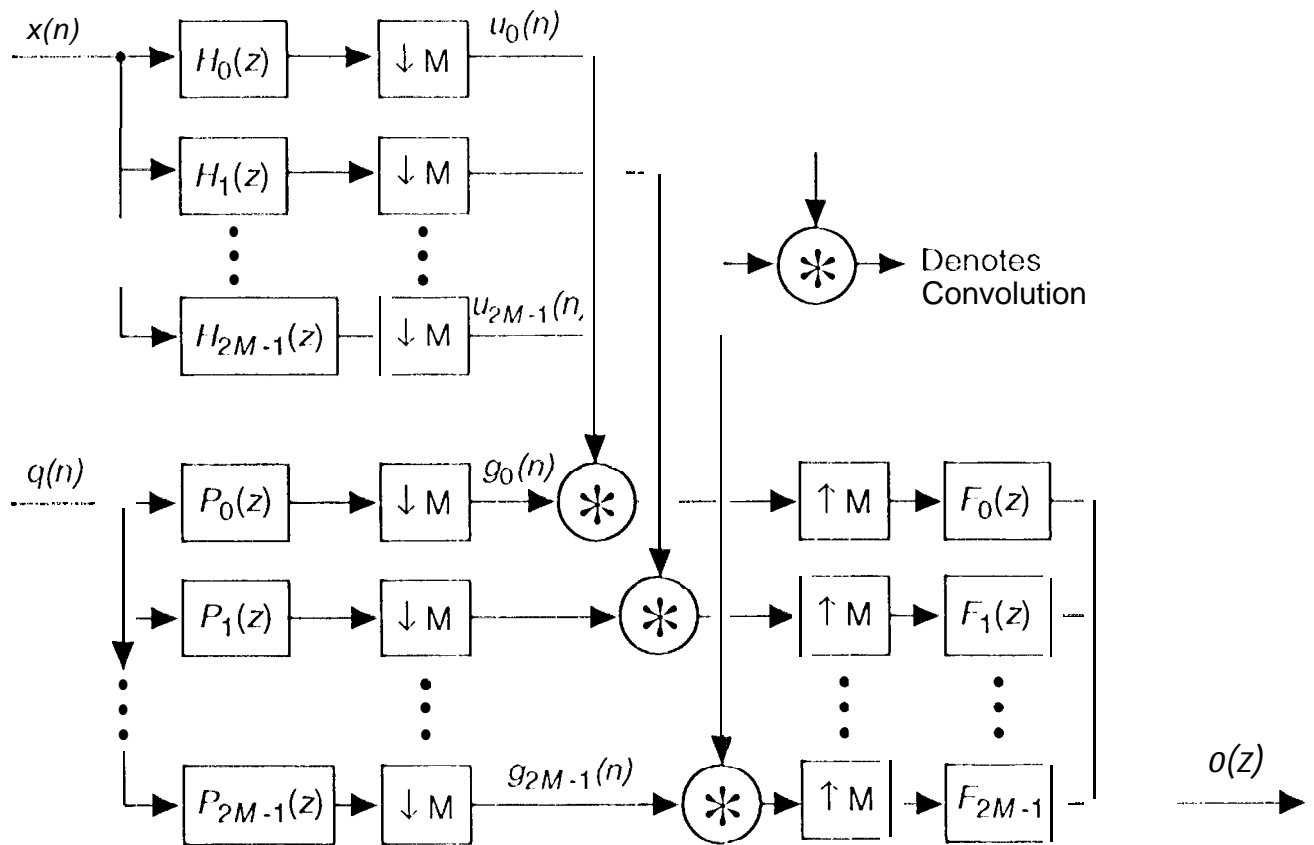


Figure 2. Subband Convolution

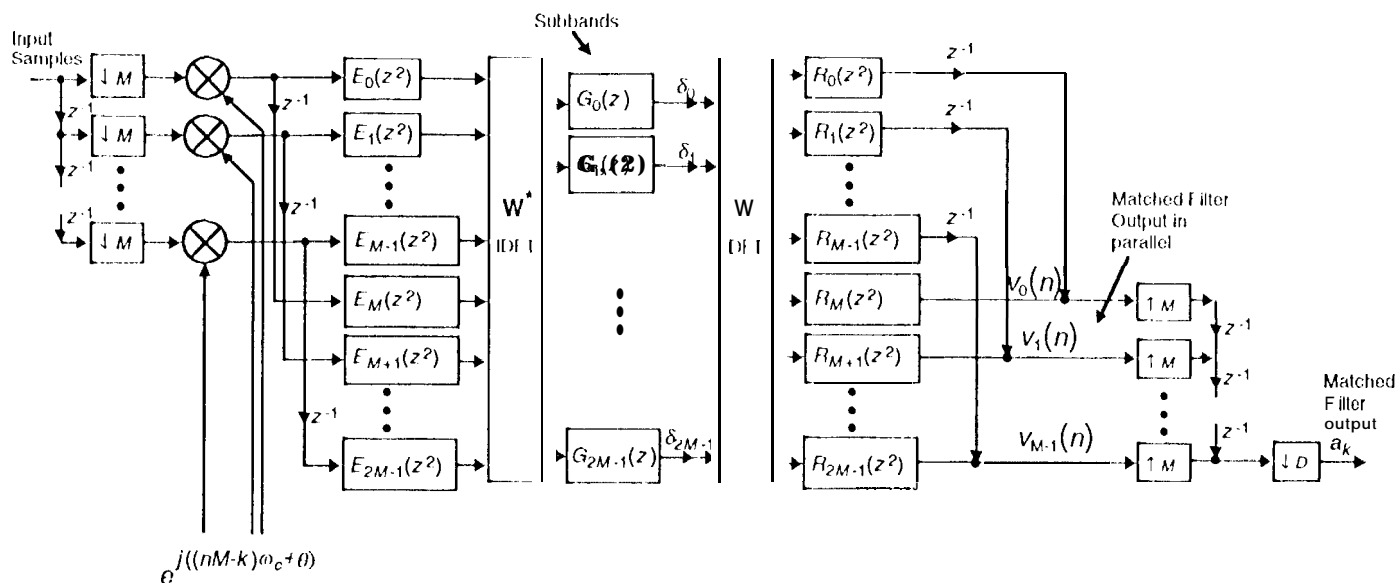


Figure 3. PRX block diagram

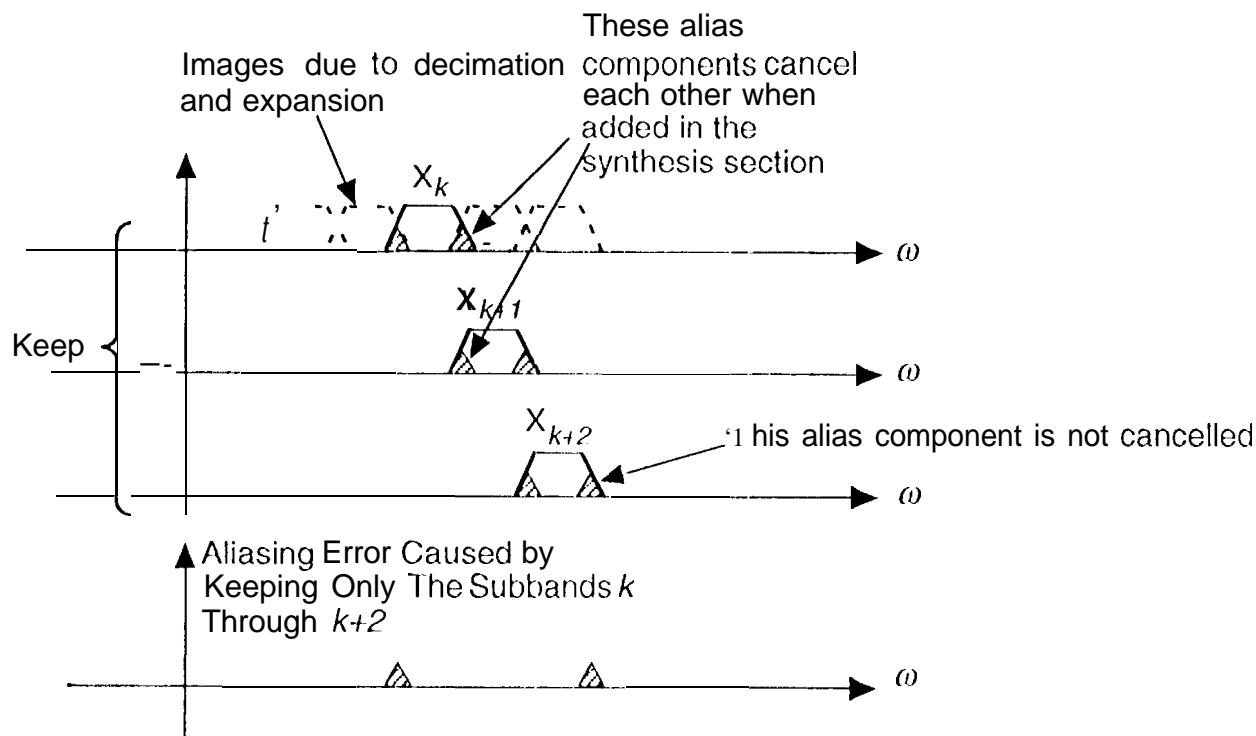
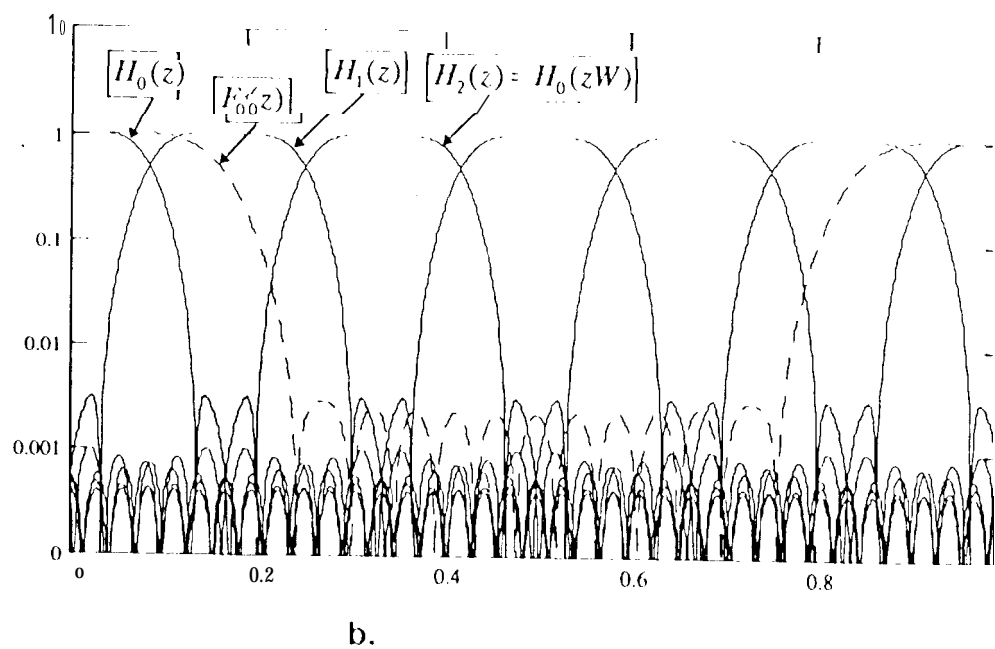
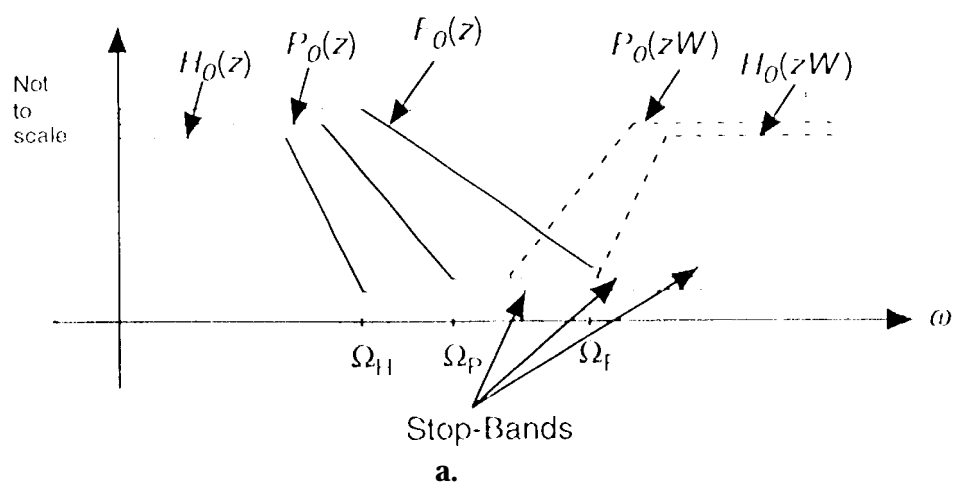


Figure 4. Aliasing Error Due to Dropping of Synthesis Filters



**Figure 5. Filter Design: a.Specifications (The Case Of $\Omega_{fl} < \Omega_p < \Omega_f$),
b. A Design Example for $M=3$**

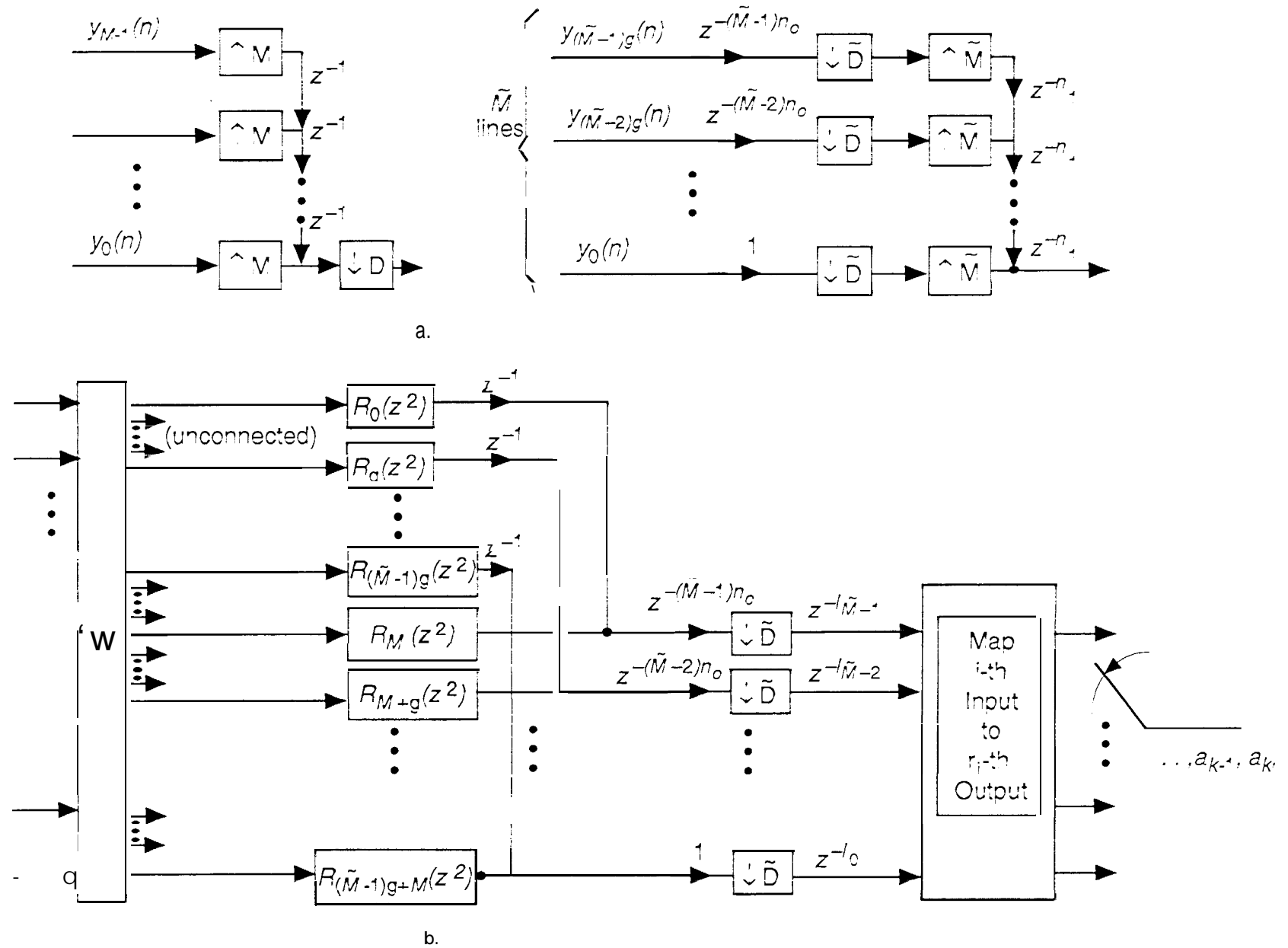


Figure 6. Symbol Stream Generation from the Parallel Output (a) Rearranging the PRX output (b) Resulting PRX output section

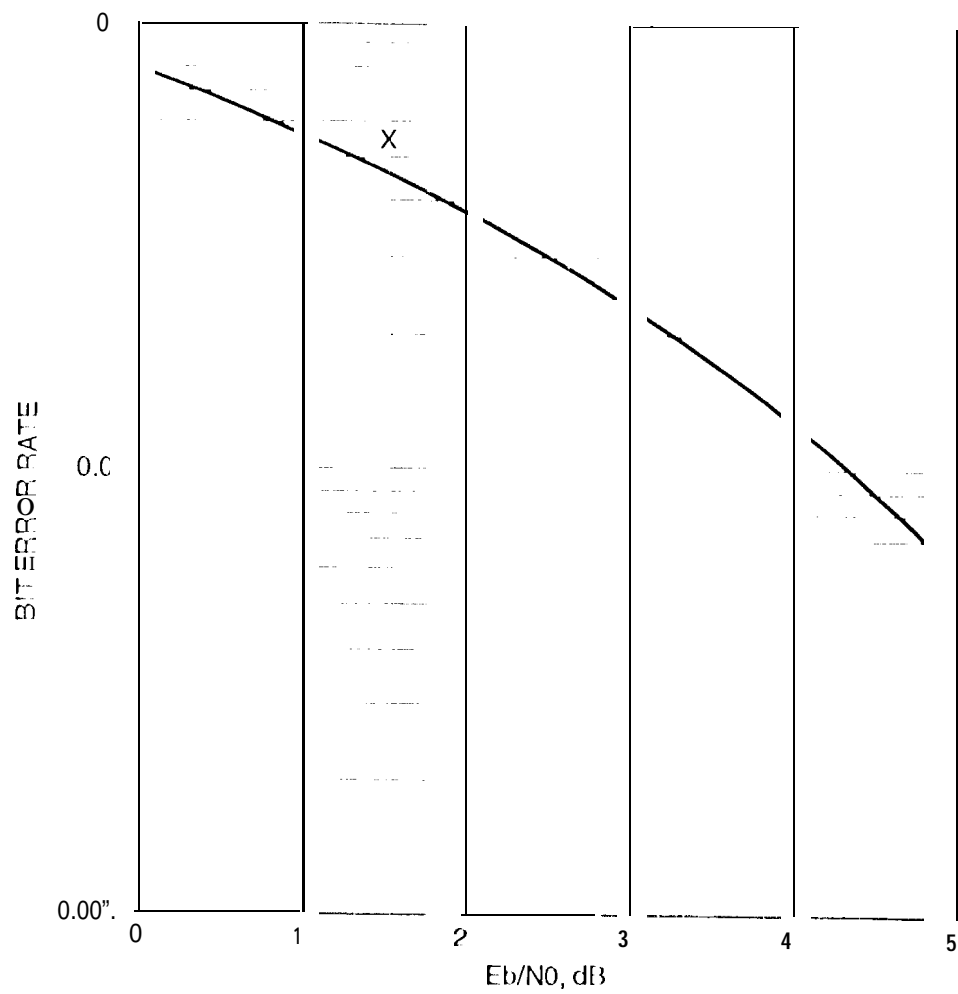


Figure 7. BER Performance of Filter-bank Receiver With 4 Samples Per Symbol and IF Sampling

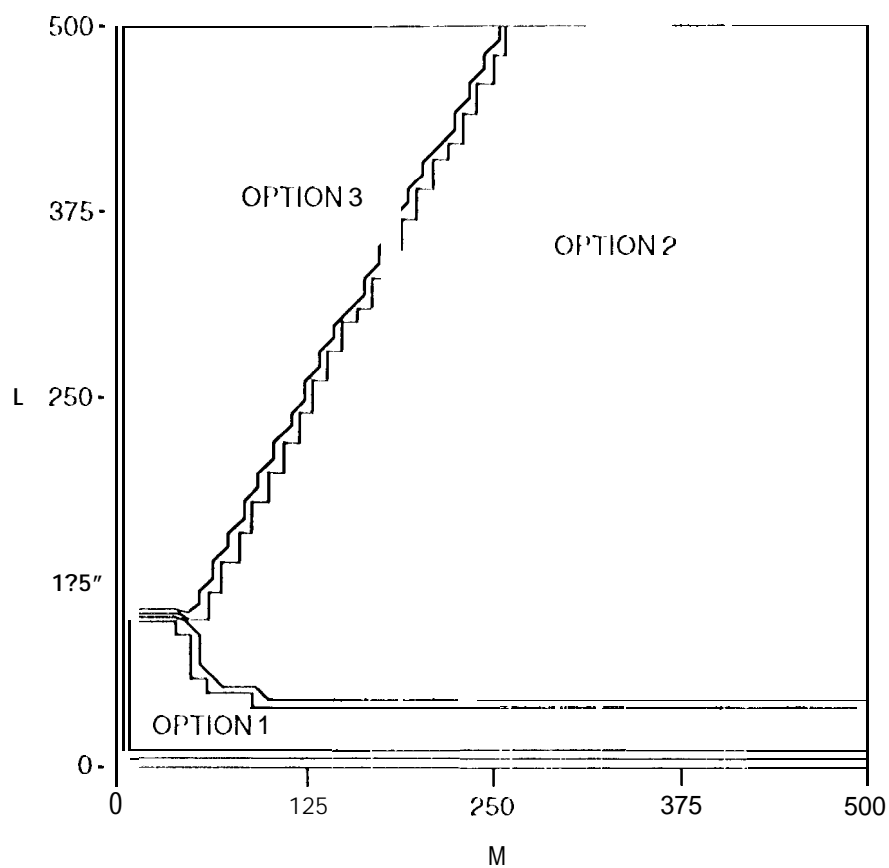


Figure 8. Complexity of Various Options for parallelization of Filtering Operation v.s. 1. (Filter Order) and M(Number of Banks)